The variations of VOCs based on the policy change of Omicron in traffic-hub city Zhengzhou

Bowen Zhang[1, 3], Dong Zhang[2, 3], Zhe Dong[2, 3], Xinshuai Song[1, 3], Ruiqin Zhang[1, 3], Xiao Li[1, 3,*]

[1]School of Ecology and Environment, Zhengzhou University, Zhengzhou 450001, China

[2]College of Chemistry, Zhengzhou University, Zhengzhou 450001, China

[3]Institute of Environmental Sciences, Zhengzhou University, Zhengzhou 450001, China

Correspondence to: Xiao Li, E-mail address: lixiao9060@zzu.edu.cn

Abstract: Online volatile organic compounds (VOCs) were monitored before and after the Omicron policy change at an urban site in polluted Zhengzhou from December 1, 2022, to January 31, 2023. The characteristics and sources of VOCs were investigated. The daily mean concentrations of $PM_{2.5}$ and total VOCs (TVOCs) ranged from 53.5 to 239.4 μg/m³ and 15.6 to 57.1 ppbv, respectively, with mean values of 111.5 ± 45.1 μg/m³ and 36.1 ± 21.0 ppbv, respectively, throughout the period. Two severe pollution events (designated as Case 1 and Case 2) were identified in accordance with the National Ambient Air Quality Standards (NAAQS) (China's National Ambient Air Quality Standards (NAAQS) from 2012). Case 1 (December 5 to December 10, $PM_{2.5}$ daily mean = 142.5 μg/m³) and Case 2 (January 1 to January 8, $PM_{2.5}$ daily mean = 181.5 μg/m³) occurred during the infection period (when the policy of "full nucleic acid screening measures" was in effect) and the recovery period (after the policy was cancelled), respectively. The $PM_{2.5}$ and TVOCs values for Case 2 are, respectively, 1.3 and 1.8 times higher than those for Case 1. The results of the positive matrix factor modeling demonstrated that the primary source of volatile organic compounds (VOCs) during the observation period was industrial emissions, which constituted 32% of the total VOCs, followed by vehicle emissions (27%) and combustion (21%). In Case 1, industrial emissions constituted the primary source of VOCs, accounting for 32% of the total VOCs. In contrast, in Case 2, the contribution of vehicular emission sources increased to 33% and became the primary source of VOCs. The secondary organic aerosol formation potential for Case 1 and Case 2 were found to be 37.6 μg/m³ and 65.6 μg/m³, respectively. In Case 1, the largest contribution of SOAP from industrial sources accounted for the majority (63%, 23.8 μg/m³), followed by vehicular sources (18%).

After the end of the epidemic and the resumption of productive activities in the society, the difference in the proportion of SOA generated from various sources decreased. Most of the SOAP came from solvent use and fuel evaporation sources, accounting for 32% (20.9 μg/m³) and 26% (16.8 go/m³), respectively. On days with minimal pollution, industrial sources and solvent use remain the main contributors to SOA formation. Therefore, regulation of emissions from industry, solvent-using industries and motor vehicles need to be prioritized to control the $PM_{2.5}$ pollution problem.

Keywords: Volatile organic compounds; Pollution episode; Source apportionment; Positive Matrix Factorization model; Secondary organic aerosol formation potential;

1. Introduction

Volatile organic compounds (VOCs) in the atmosphere have high reactivity and can react with nitrogen oxides (NO_x) to form a series of secondary pollutants such as ozone (O_3) and secondary organic aerosol (SOA), resulting in regional air pollution (Li et al., 2019; Hui et al., 2020). The problem of O_3 pollution has been plaguing major urban agglomerations in China (Zheng et al., 2010; Li et al., 2014; Wang et al., 2017). SOA is an important component of fine particulate matter ($PM_{2.5}$) and contributes significantly to haze pollution (Liu et al., 2019). $PM_{2.5}$ remains the most significant air pollutant in many Chinese cities for years (Shao et al., 2016; Wu et al., 2016). In addition, VOCs, represented by the benzene homologues, can cause damage to kidneys, liver, and nervous system of humans when they enter the body (Zhang et al., 2018).

Studies have shown that the most common VOC components in China are alkanes, olefins, aromatic hydrocarbons, oxygenated VOCs (OVOCs), and halogenated hydrocarbons, among which alkanes are the most abundant species (Liu et al., 2020; Zhang et al., 2021a). VOCs in the atmosphere have a wide range of sources, and VOCs in different regions are affected by multiple factors such as local geography, climate, and human activities (Mu et al., 2023; Zou et al., 2023). The above reasons lead to significant regional and seasonal differences in the characteristics of VOCs (Song et al., 2021). For example, the annual average concentration of VOCs in the coastal background area of the Pearl River Delta is 9.3 ppbv. The seasonal variation trend of VOCs is high in autumn and winter and low in summer (Yun et al., 2021). In contrast, the average VOC concentration in autumn and winter in Beijing was 22.6 ± 12.6 ppbv, and the VOC concentration in the winter heating period was twice that in the autumn non-heating period (Niu et al., 2022).

Moreover, the sources of VOC components in different regions are also related to the local industrial structure and living habits. In rural areas of North China Plain in winter, it is found that the SOA formation potential (SOAP) of VOCs under low NO_x conditions is significantly higher than that under high NO_x conditions, and the increase of aromatic hydrocarbon emissions caused by coal combustion is the main reason for the higher SOAP in winter (Zhang et al., 2020). Li et al. (2022) found that the average increased concentration of acetylene was 4.8 times from autumn to winter in the Guanzhong Plain, indicating that fuel combustion during the heating period in winter has a significant impact on the composition of VOCs. In contrast, continuous

observations conducted by Zhou et al. (2022) in the suburbs of Dongguan in summer found that industrial solvent usage, liquefied petroleum gas (LPG) and oil and gas volatilization were the main sources of VOCs. The results highlighted a wide variation of characteristics, sources and chemical reactions of VOCs in the atmosphere thus it is necessary to investigate VOCs in different cities when formulating control measures.

Zhengzhou, as the capital of Henan Province, is an important transportation hub and economic center in the Central Plains region. Zhengzhou is currently facing significant air pollution problems, with the Air Quality Index at the bottom of the national ranking of 168 cities for many years. In January 2023, for example, the number of polluted days with $PM_{2.5}$ as the primary pollutant was 17, and the daily average value of $PM_{2.5}$ reached a maximum of 298 $\mu g/m^3$ (https://www.aqistudy.cn/historydata/daydata.php?city=%E9%83%91%E5%B7%9E&month=202301, Accessed Jan 2024), which is almost 300% higher than the Chinese daily average standard (grade II, 75 $\mu g/m^3$). The studies of VOCs were carried out in Zhengzhou in recent years, which focused on the characteristics and sources of VOCs during pollution episodes (Lai et al., 2024) or before the coronavirus epidemic outbreak (Li et al., 2020; Zhang et al., 2021b). While some atmospheric VOCs studies involving the impact of Covid-19 lockdown have been performed in India (Singh et al., 2023a), in China (e.g., Pei et al., 2022; Jensen et al., 2023; Zuo et al., 2024), or with respect to toluene, benzene, m/p-xylene and ethylbenzene only (e.g., Sahu et al., 2022; Singh et al., 2023b), a gap persisted in the investigation of VOCs due to the impact of abolishment of China's zero-policy. Furthermore, some studies have discussed the impact of changes in human production activities on air pollution during and after the outbreak of the coronavirus disease (e.g., Ma et al., 2022; Jiang et al., 2023; Song et al., 2023), but as mentioned earlier, only a few studies with in-depth exploration of the changes in VOCs and none dealing with ending the zero-Covid policy during Omicron variant infection period.

In this study, we conducted continuous online observations of VOCs during the polluted winter season at an urban site in Zhengzhou. The study covered the period following the removal of lockdown measures. We focused on pollution events when the daily average $PM_{2.5}$ concentration exceeded 75 $\mu g/m^3$ (China's Class II standard) for more than three consecutive days. Days with $PM_{2.5}$ concentrations below 35 $\mu g/m^3$ (China's Class I standard) were classified as clean days. During this period, China lifted zero-COVID strategies, announcing the '10 measures' for optimizing COVID-19 rules

on December 7, 2022 (http://www.news.cn/politics/2022-12/07/c_1129189285.htm, Accessed Jan 2024). Zhengzhou's epidemic prevention and control measures changed with the issuance of Circular No. 163 on December 4, 2022, which allowed the reopening of closed public places. As a result, movement within Zhengzhou increased and social production resumed. Our research specifically examines the period dominated by the COVID-19 Omicron variant. where they demonstrate notable differences from the early virus strains (i.e., original SARS-CoV-2 virus and Delta) in terms of geographical transmission, the scale of the infected population, and symptom manifestation (Petersen et al., 2022; Merino et al., 2023).

After the quarantine policy was lifted, people basically rested at home due to infection or fear of infection with Omicron. The resumption of normal production and life depends on herd immunization. This outbreak event is the longest in duration and the largest in number of infections since the 2020 outbreak of the novel coronavirus in Zhengzhou. It would be beneficial to investigate the impact of this event on emissions related to transportation and industrial production. This change is worth exploring in terms of its impact on transportation and industrial production emissions. Therefore, the characteristics and variations of VOCs during different periods were investigated to assess their impact on the formation of SOA and to provide data support for future pollution control policies in Zhengzhou.

2. Materials and methods

2.1 Sample collection and Chemical analysis

The online VOCs observation station is located on the roof of the Zhengzhou Environmental Protection Monitoring Center, which is in the urban area. The sampling site is close to main roads on three sides (150 m away from Funiu Road on the east side, 200 m away from Qinling Road on the west side, and connected to Zhongyuan Road on the south side), and surrounded by residential areas and commercial areas without other large nearby stationary sources. The sampling period for this study was from December 1, 2022, to January 31, 2023, and serious $PM_{2.5}$ pollution in Zhengzhou was of frequent occurrence during December and January. (https://www.aqistudy.cn/historydata/monthdata.php?city=%e9%83%91%e5%b7%9e#:~:text=%E7%94%9F%E5%91%BD%E6%9D%A5%E6%BA%90%E8%87%AA%E7%84%B6%EF%BC%8C%E5%81%A5). Apart from a brief occurrence of rain and snow on December 25, the sampling days were either sunny or cloudy. The wind speed (WS), temperature (Temp) and relative humidity (RH) during this period were 1.3 ± 0.9 m/s, 5.3 ± 3.2 ℃ and 38.9 ± 19.0%), respectively, similar to the values observed in previous years in Zhengzhou. It is interesting to point out that the sampling period in the present study covered the entire infection period of Omicron in Zhengzhou, including the phase of surge in infected population (Infection period, from 2022.12.01 to 2022.12.31) and restoration of production and livelihood phase (Recovery period, from 2023.1.1 to 2023.1.31 in 2023) (Fig. S1, Chinese Center for Disease Control and Prevention, 2023).

The VOCs were measured hourly using a GC-FID/MS (TH-PKU 300 b, Wuhan Tianhong Instruments Co., China). The instrument TH-PKU300b includes electronic refrigeration ultra-low temperature pre-concentration sampling system, analysis system and system control software. The ambient VOCs in the first 5 minutes of each hour were collected by the sampling system and then entered the concentration system. Under low temperature conditions, the VOCs samples collected were frozen in the capillary capture column, and then quickly heated and resolved, so that the compounds entered the analysis system. After separation by chromatographic column, the compounds were monitored by FID and MS detectors. During the detection process, the atmospheric samples collected undergo analysis through two distinct pathways. C2-C5 hydrocarbons are analyzed using FID, while C5-C12 hydrocarbons, halocarbons,

and OVOCs are analyzed with a MS detector. After excluding species with missing data exceeding 10%, the detected volatile organic compounds include 29 alkanes, 11 alkenes, 17 aromatics, 35 halocarbons, 12 OVOCs, 1 alkyne (acetylene), and 1 sulfide (CS_2) with a total of 106 compounds. A detailed description of the instrumentation can be found in our previous study (Zhang et al., 2021b; Shi et al., 2022; Zhang et al., 2024).

The instrument was calibrated per week to ensure the accuracy of VOCs by injecting standard gases with a five-point calibration curve. The detection limit of C2-C5 hydrocarbons ranges from 0.007 to 0.099 ppbv, other hydrocarbons are 0.004–0.045 ppbv, halogenated hydrocarbons 0.009-0.099 ppbv, OVOCs and other compounds of 0.006–0.095 ppbv. Thirty-two of the monitored VOCs had over 90% observed data greater than the detection limit, and 34 had more than 50% observed data greater than the detection limit.

Simultaneous observations at the same site were also carried out for particulate matter ($PM_{2.5}$, PM_{10}), other trace gases (carbon monoxide (CO), O_3, nitric oxide (NO), nitrogen dioxide (NO_2)), and meteorological data (Temperature, RH, WS, and wind direction (WD)) based on 1 h resolution.

2.2 Positive Matrix Factorization (PMF) model

EPA PMF5.0 model was used for the quantitative source analysis of VOCs (Norris et al., 2014). The principles and methods have been described in detail in previous studies (Mozaffar et al., 2020; Zhang et al., 2021b). The decomposition of the PMF mass balance equations is simplified as follows (Norris et al., 2014):

$$x_{ij} = \sum_{k=1}^{p} g_{ik}\, f_{kj} + e_{ij} \qquad (1)$$

where x_{ij} is the mass concentration of species j measured in sample i; g_{ik} is the contribution of factor k to the sample i; f_{kj} represents the content of the jth species in factor k; e_{ij} is the residual of species j in sample i; p represents the number of factors. The fitting objective of the PMF model is to minimize the function Q to obtain the factor contributions and contours. The formula for Q is given in Eq. (2):

$$Q = \sum_{i=1}^{n}\sum_{j=1}^{m}\left[\frac{x_{ij} - \sum_{k=1}^{p} g_{ik} f_{kj}}{u_{ij}}\right]^2 \quad (2)$$

where n and m denote the number of samples and VOC species, respectively.

Concentrations and uncertainty data are required for the PMF model. In this study, the median concentration of a given species is used to replace missing values with an uncertainty of four times of the median values; data less than the Method Detection Limit (MDL) were replaced with half the MDL, with an uncertainty of 5/6 of the MDL; and the uncertainty for values greater than the MDL was calculated using Eq. (3). In Eq. (3), EF is error fraction, expressed as the precision of VOCs species, and the setting range can be adjusted from 5 to 20% according to the concentration difference (Buzcu et al., 2006; Song et al., 2007); and c_{ij} is the concentration of species *j* in sample *i*:

$$U_{ij} = \sqrt{\left(EF \times c_{ij}\right)^2 + (0.5 \times MDL)^2} \quad (3)$$

when the concentration of VOCs in the species is less than the value of the detection limit U_{ij} is calculated using Eq. (4):

$$U_{ij} = \left(\frac{5}{6}\right) MDL \quad (4)$$

VOC species and concentration input into PMF were carefully selected to ensure the accuracy of the PMF results. Species were excluded when over 25% of the samples were missing or concentrations values were below the MDL (Gao et al., 2018); VOCs with a short lifetime in the atmosphere were also excluded unless they are source-relative species (Zhang et al., 2014; Shao et al., 2016). After that, retained VOC species were categorized according to the signal-to-noise ratio (S/N) with S/N < 0.2 species categorized as bad, 0.2 < S/N < 2 species categorized as weak; and S/N > 2 species categorized as strong (Shao et al., 2016).

We used displacement of factor elements (DISP) to assess PMF modelling uncertainty (for a description, see Paatero et al. (2014)). Q was less than 1% and no swaps occurred for the small est dQ^{max} in DISP. Fpeak values from -2 to 2 were tested to explore the rotational stability of the solutions. Q_{true}/Q_{exp} is lowest when Fpeak = 0, so we chose the PMF results for that case (Fig. S2a). After examining 3-8 factors, 20 base runs with 5 factors eventually selected to represent final result. We provide an explanation of factor selection in the supplementary materials. Fig. S2(b) includes Q_{true}/Q_{exp}, Q_{robust}/Q_{exp} for factors 3-8. The slopes of these two ratios in changed at five

factors, and we found that five factors were more realistic after repeated comparisons of the results at four, five and six factors.

2.3 SOA generation potential

The contributions of VOC species to SOAP were calculated based on the toluene weighted mass contributions (TMC) method (Derwent et al., 2010). The methodology for calculating SOAP is as follows:

$$SOAPF_i = \frac{VOCs\ component\ i\ to\ SOA\ mass\ concentration\ increments}{Toluene\ to\ SOA\ mass\ concentration\ increment} \times 100 \quad (5)$$

$SOAPF_i$ for each VOC is taken from the literature (Derwent et al., 2010). The SOAP was estimated by multiplying the $SOAPF_i$ value by the concentration of individual VOC species. The SOAP calculations through each VOC are as follows:

$$SOAP = \sum E_i \times SOAPF_i \quad (6)$$

E_i is the concentration of species i.

3. Results and discussion

3.1 Overview of variation in pollutants and meteorological parameters

Figure 1 shows the time series of meteorological parameters, TVOCs, O_3, NO_x, SO_2, CO and $PM_{2.5}$ during the observed periods. Low WS and Temperature were found with an average value of 1.3 ± 0.6 m/s and 5.0 ± 2.5 °C, respectively, during the entire period, comparable with observations at the same site in 2021 (Lai et al., 2024). A total of 62 days of valid data was acquired with the daily average concentration of $PM_{2.5}$ ranging from 53 to 239 μg/m^3, with the average value of 111 ± 45 μg/m^3. The concentration of TVOCs ranged from 15.6 to 57.1 ppbv with an average of 36.1 ± 21.0 ppbv, higher than the same period in last year (27.9 ± 12.7 ppbv, Lai et al., 2024). During the observation period, the average values of T, WS and RH were 5.0 ± 2.5 °C, 1.3 ± 0.6 m/s and 38.9 ± 16.7%, respectively.

Previous studies have shown that meteorological factors such as low WS, high RH,

and low precipitation are responsible for the increase in $PM_{2.5}$ pollution in Zhengzhou in winter (Duan et al., 2019). Our analysis of the correlation between different pollutants and meteorological conditions during the pollution period showed that $PM_{2.5}$, TVOCs and NO_x were positively correlated with relative humidity (Fig. S3), which is consistent with the results of some previous studies (Wang et al., 2019). Yu et al. (2018) identified RH and WS as the most influential meteorological conditions of $PM_{2.5}$ during winter. Their findings revealed a positive correlation between hourly $PM_{2.5}$ concentrations and RH ($r = 0.84$, $p < 0.01$) and a negative correlation between $PM_{2.5}$ concentrations and WS ($r = -0.62$, $p < 0.01$). The WS and RH between the infection and recovery periods were similar in this study which were largely considered to be of the same type of weather (Yu et al., 2018). However, the mean $PM_{2.5}$ concentration during the recovery period was found to be 1.6 times higher than that observed during the infection period. Furthermore, the concentrations of other pollutants (including SO_2, NO_2, CO, and O_3) exhibited analogous trends during the infection and recovery periods. The concentration of TVOCs during the recovery period was 1.2 times higher than that during the infection period, exhibiting a significant upward trend following the resumption of production. It is notable that WS, which is only 0.3 m/s higher in Case 1 than in Case 2, and RH, which is 13% higher in Case 1 than in Case 2, were relatively stable, while the concentration of pollutants is significantly higher in Case 2 than in Case 1. This is presumably attributable to the resumption of production activities in Case 2, which resulted in a notable increase in emissions. Decreased trends of air pollutants were found in other studies before and after the outbreak of the novel coronavirus (COVID-19) in early 2020 (Qi et al., 2021; Wang et al., 2021).

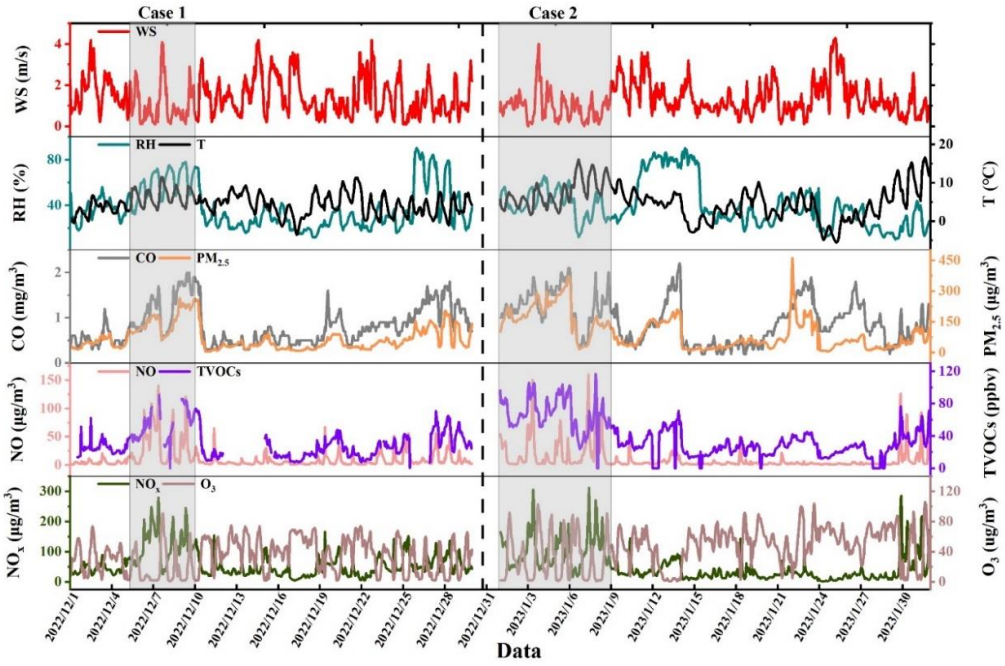

Fig. 1. Time series of WS, T, RH, CO, $PM_{2.5}$, NO, TVOCs, NO_x and O_3 during the observation period.

The shadow section in Fig. 1 represents two haze pollution events during the monitoring period. A pollution event is determined when the daily average concentration of $PM_{2.5}$ exceeds 75 μg/m^3 (China's II-level standard) for at least three consecutive days. Case 1 (December 5 to December 10 with daily average $PM_{2.5}$ = 142.5 μg/m^3) and Case 2 (January 1 to January 8 with daily average $PM_{2.5}$ = 181.5 μg/m^3) were selected as they represent the pollution events in infection and recovery periods, respectively, due to their long duration and high pollution levels. Any day with a $PM_{2.5}$ concentration lower than 35 μg/m^3 (China's I-level standard) is considered as Clean day.

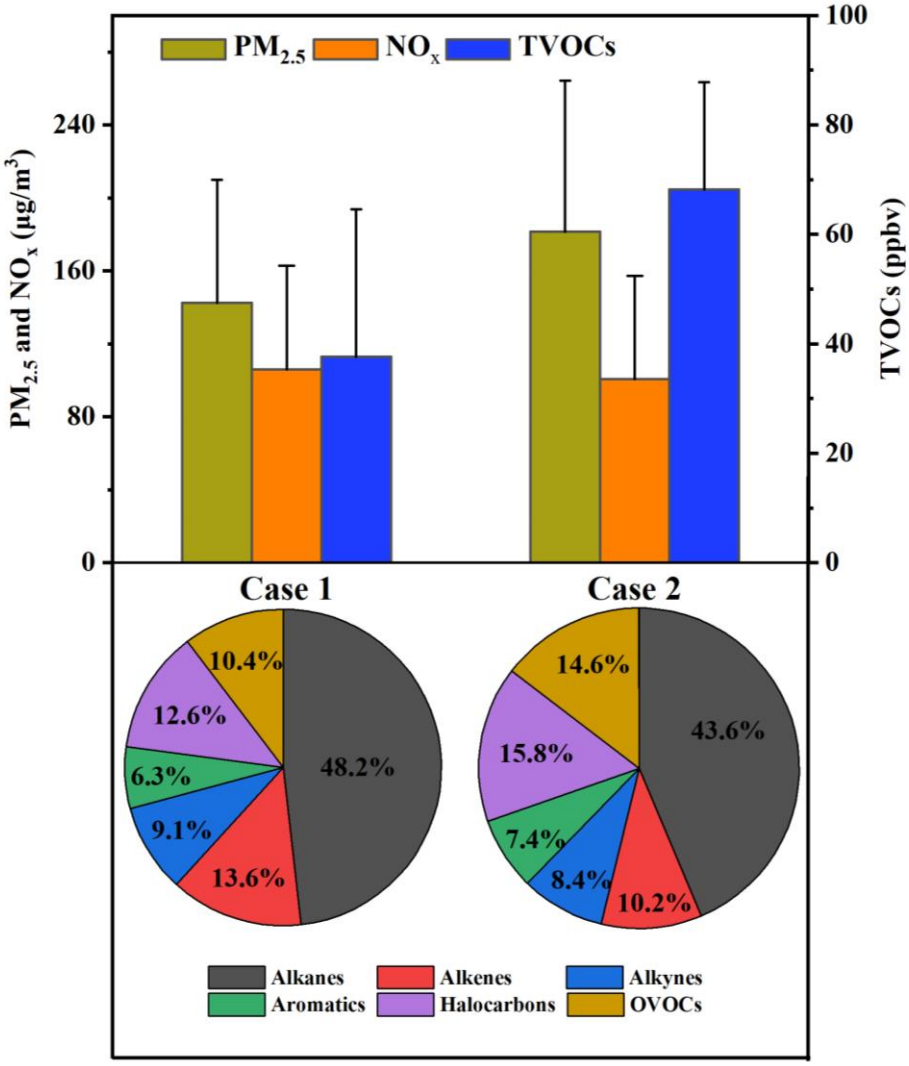

Fig. 2. The concentration of $PM_{2.5}$, NO_x, TVOCs and the composition ratio of VOCs in Case 1 and Case 2.

As for the two representative pollution processes (Case 1 during the infection period and Case 2 during the recovery period), the concentration of TVOCs in Case 1 and Case 2 were 48.4 ± 20.4 and 67.6 ± 19.6 ppbv (Fig. 2), respectively, increased by 63% and 188% compared with values during clean days. The average concentrations of $PM_{2.5}$ and TVOCs during Case 2 were 1.3 and 1.8 times the values in Case 1. The highest volume contributions of alkanes were found both in Case 1 (48%) and Case 2 (44%), consistent with the results in the Yangtze River Delta region (36-43%, Liu et al., 2023). While alkenes exhibited higher volume percentages of 13% in Case 1, followed by halogenated hydrocarbon (12%) and OVOCs (10%). Higher volume percentages of alkanes and alkenes in Case 1 were similar to the results in the gasoline evaporation site in winter (Niu et al., 2022). Equivalent volume contribution of halogenated hydrocarbon and OVOCs (15%) were found in Case 2, followed by alkenes (10%).

Although aromatic hydrocarbons have the lowest volumetric contribution (6% in Case 1 and 7% in Case 2), they show the largest increase from clean days to pollution.

Table 1 The average concentrations of meteorological parameters and pollutants during different processes.

Category	Entire process (2022.12.1-2023.1.31)	Infection period (2022.12.1-2022.12.31)	Recovery period (2023.1.1-2023.1.31)	Case 1 (2022.12.5-2022.12.10)	Case 2 (2023.1.1-2023.1.8)	Clean Days
	N = 62 days	N = 31 days	N = 31 days	N = 6 days	N = 8 days	N = 8 days
WS (m/s)	1.3 ± 0.6	1.4 ± 0.6	1.3 ± 0.6	1.2 ± 0.9	0.9 ± 0.7	1.4 ± 0.8
T (°C)	5.0 ± 2.5	4.7 ± 1.7	5.4 ± 3.1	6.1 ± 2.2	7.4 ± 3.5	4.1 ± 3.0
RH (%)	38.9 ± 16.7	37.6 ± 15.5	40.2 ± 18.2	55.7 ± 14.7	42.0 ± 12.1	29.5 ± 18.1
TVOCs (ppbv)	36.1 ± 21.0	31.9 ± 18.1	39.8 ± 22.4	37.6 ± 27.0	68.2 ± 19.6	22.7 ± 11.1
SO_2 (μg/m^3)	11.4 ± 2.7	10.2 ± 2.8	12.7 ± 2.3	11.0 ± 3.7	16.2 ± 6.1	6.5 ± 2.5
NO_2 (μg/m^3)	47.2 ± 10.0	46.8 ± 8.6	47.8 ± 11.7	62.7 ± 20.5	65.0 ± 21.3	20.8 ± 15.9
CO (mg/m^3)	0.9 ± 0.2	0.8 ± 0.2	1.1 ± 0.2	1.2 ± 0.5	1.3 ± 0.4	0.5 ± 0.2
O_3 (μg/m^3)	34.9 ± 6.0	31.1 ± 4.5	39.0 ± 4.6	21.8 ± 23.7	32.5 ± 29.6	52.6 ± 18.4
$PM_{2.5}$ (μg/m^3)	111.5 ± 45.1	86.6 ± 34.6	138.3 ± 39.6	142.5 ± 67.4	181.5 ± 82.7	23.8 ± 16.8

Table 2 Concentration of VOC species during different processes (ppbv).

Category	Entire process	Infection period	Recovery period	Case 1	Case 2	Clean days
TVOCs	36.1 ± 21.0	31.9 ± 18.1	39.8 ± 22.4	48.4 ± 20.4	67.6 ± 19.6	17.5 ± 9.5
alkanes	16.8 ± 9.2	15.0 ± 8.4	18.4 ± 9.5	23.1 ± 10.0	29.5 ± 8.4	9.2 ± 5.6
alkenes	4.1 ± 2.7	3.8 ± 2.6	4.4 ± 2.7	6.5 ± 2.9	7.0 ± 2.6	1.7 ± 1.3
alkynes	3.1 ± 2.0	2.7 ± 1.7	3.4 ± 2.1	4.3 ± 2.0	5.8 ± 1.9	1.3 ± 0.8
aromatics	2.1 ± 2.0	1.8 ± 1.5	2.3 ± 2.2	3.0 ± 1.8	4.9 ± 2.8	0.7 ± 0.5
halogenated hydrocarbon	5.4 ± 3.3	4.4 ± 2.3	6.2 ± 3.8	6.0 ± 1.9	10.7 ± 3.6	2.7 ± 1.4
OVOCs	4.6 ± 3.2	3.5 ± 2.7	5.1 ± 3.5	5.0 ± 2.4	9.7 ± 2.8	1.9 ± 1.1

3.2 Source Analysis of VOCs

Specific VOC ratios can be used for initial source identification of VOCs and determination of photochemical ages of air masses (Monod et al., 2001; An et al., 2014; Li et al., 2019). In this study, the ratios of toluene/benzene (T/B), isopentane/n-pentane, isobutane/n-butane, and m/p-xylene/ethylbenzene (X/E) were selected to initially identify the potential sources of VOCs (Fig. 3). Concentrations of selected pollutants and ratios used are shown in Table S1.

The toluene-to-benzene ratio (T/B ratio) was widely used to assess the relative importance of different sources. Specifically, T/B ratio with a value of 1.3-3.0 was observed in vehicle emissions for vehicles with different fuel types (Schauer et al., 2002; Wang et al., 2015). The reported T/B ratio for combustion processes was between 0.13 and 0.7 (Li et al., 2011; Wang et al., 2014). The mean value of T/B ratio for the entire period was 1.0, with the majority of the data (99%) falling between 0.1 and 3.0 and concentrated within the 0.7-1.3 range (49%). This suggests that both traffic emissions and combustion are significant sources of VOCs.

The isopentane/n-pentane concentration ratios of 0.6-0.8 represent mainly coal combustion emissions, ratios of 0.8-0.9 represent LPG emissions, 2.2-3.8 represent vehicle exhaust emissions, and 1.8-4.6 represent fuel evaporation (Conner et al., 1995; Liu et al., 2008; Li et al., 2019). The sources of isopentane and n-pentane in this study were intricate and multifaceted. The mean isopentane/n-pentane ratio was 1.4, with the majority of data points (99%) falling within the range of 0.1-4.6, with a notable concentration in the 0.8 to 1.8 interval. This indicates that pentane is influenced by a combination of emissions from LPG and fuel evaporation.

Isobutane/n-butane concentration ratios of 0.2-0.3 represent vehicle emissions, 0.4-0.6 represent LPG usage, and 0.6-1.0 represent natural gas emissions (Russo et al., 2010; Zheng et al., 2018). The mean isobutane/n-butane ratio in this study was 0.5, with the majority of data points (99%) falling within the 0.4-0.6 range, indicating that VOCs at the observation sites were significantly influenced by the use of LPG. (Shao et al., 2016; Zeng et al., 2023).

The ratio of X/E can be used to infer the photochemical age of the air mass. X/E ratios around 2.5-2.9 are typical of urban areas, indicating that VOCs are mainly from the urban area (fresh air mass) (Kumar et al., 2018). When this ratio is significantly lower than 3.0, it indicates that VOCs are mainly transported from distant sources (aging air masses) (Kumar et al., 2018). The average X/E value in this study was 2.0 (Fig. 3(d)), indicating low photochemical activity and aging of the air mass at the observation site. Potential source analyses also indicate that air masses are affected by long-range transport (Fig. S4).

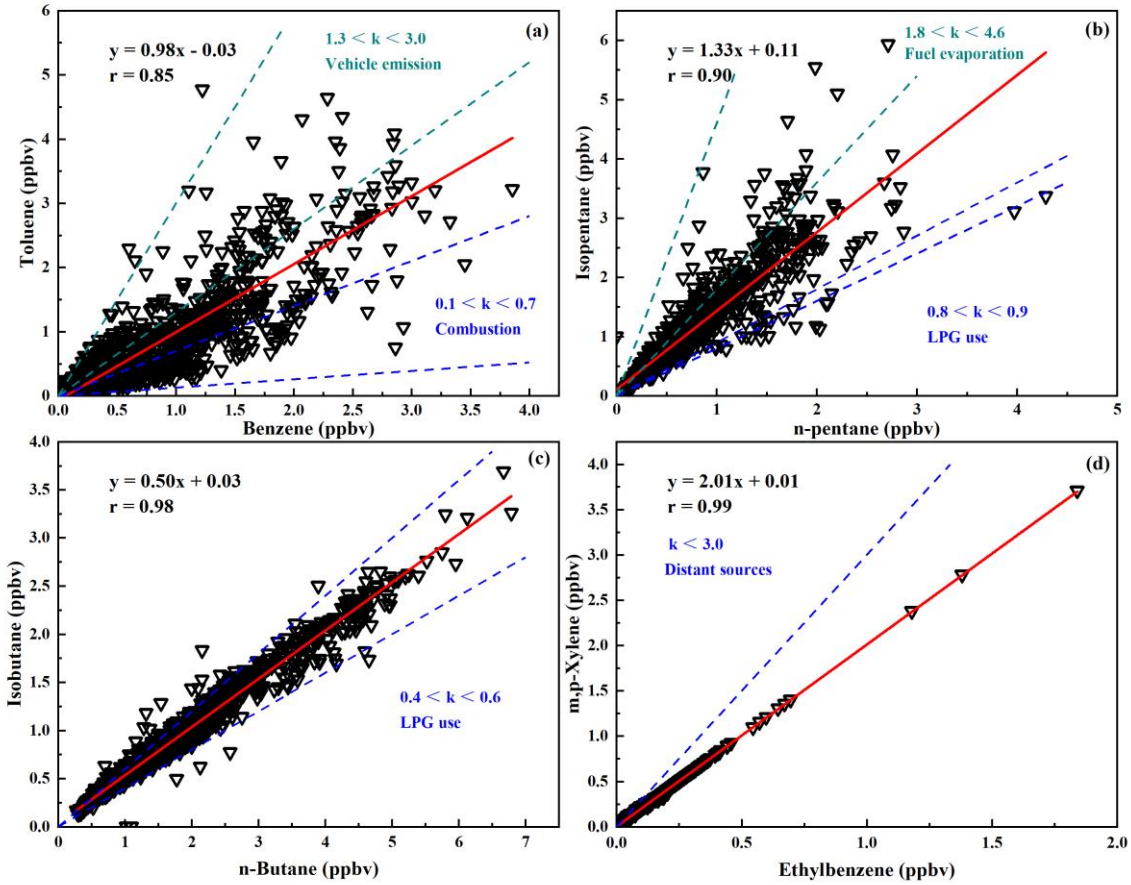

348

349 Fig. 3. Correlation analysis between specific VOC species.

350 Figure 4 shows the chemical profiles of individual VOCs resolved by the PMF
351 model during the entire observation period. These five factors eventually selected as
352 potential sources for the observed VOCs are: (1) Fuel evaporation; (2) Solvent usage;
353 (3) Vehicular emission; (4) Industrial source; and (5) Combustion. These 5 factors have
354 been commonly reported before, e.g., in Shijiazhuang, northern China (Guan et al, 2023)
355 and in Beijing (Cui et al., 2022).

356 Alkanes of C4-C6 substances were predominant in factor 1, including 2-
357 methylpentane, 3-methylpentane, isobutane, n-butane, isopentane and n-pentane from
358 oil and gas (Xiong et al., 2020). Fig. S5 shows that emissions from this source peak at
359 midday, when fuel volatilization is high, The CPF plot shows that south-east is the
360 dominant direction at wind speeds of less than 2 m/s (Fig. 5a). Therefore, factor 1 was
361 identified as the source of oil and gas volatilization.

362 The contribution of benzene, toluene, methylene chloride, 1,2-dichloroethane and
363 ethyl acetate was high in factor 2. It has been shown that benzene, toluene, ethylbenzene,
364 and xylene is an important component in the use of solvents (Li et al., 2015); methylene

chloride is often used as a chemical solvent, while esters are mostly used as industrial solvents or adhesives (Li et al., 2015). Factor 2 is determined to be solvent usage source. The CPF plot shows that due east is the main emission direction at wind speeds less than 2 m/s and southeast is the main source at wind speeds greater than 2 m/s (Fig. 5b).

Factor 3 contains predominantly C3-C8 alkanes, olefins and alkynes, and relatively high concentrations of benzene. These substances are usually emitted by industrial processes (Shao et al., 2016), so Factor 4 is defined as an industrial source. The CPF plots indicate that a local source at low wind speeds is the dominant sources (Fig. 5c).

Factor 4 is characterized by relatively high levels of C2-C6 low-carbon alkanes (ethane, propane, isopentane, n-pentane, isobutane and n-butane), olefins (ethylene and propylene), and benzene and toluene, which are important automotive exhaust tracers (Song et al., 2021; Zhang et al., 2021b). Ethylene and propylene are important components derived from vehicle-related activities. Previous studies of VOCs in Zhengzhou have shown a high percentage of VOCs emitted from gasoline vehicles, with the main source of alkanes being on-road mobile sources (Bai et al., 2020). The daily variation of this source in Fig. S5 shows a bimodal trend, with peaks occurring in the morning and evening peaks of traffic, consistent with motor vehicle emissions. Fig. 5d shows that this source is mainly from the west where wind speeds are below 2 m/s, and in this direction, there are a number of urban arterial roads with high traffic volumes. Therefore, factor 4 was defined as vehicular emission source.

The highest contribution to factor 5 is chloromethane (62%). Benzene (46%) and acetylene (41%) also contribute highly to factor 5. Chloromethane is the key tracer for biomass combustion and acetylene is the key tracer for coal combustion (Xiong et al., 2020). Therefore, factor 5 is defined as a combustion source. The CPF plot shows that at wind speeds below 2 m/s, the north-east direction is the dominant source direction (Fig. 5e).

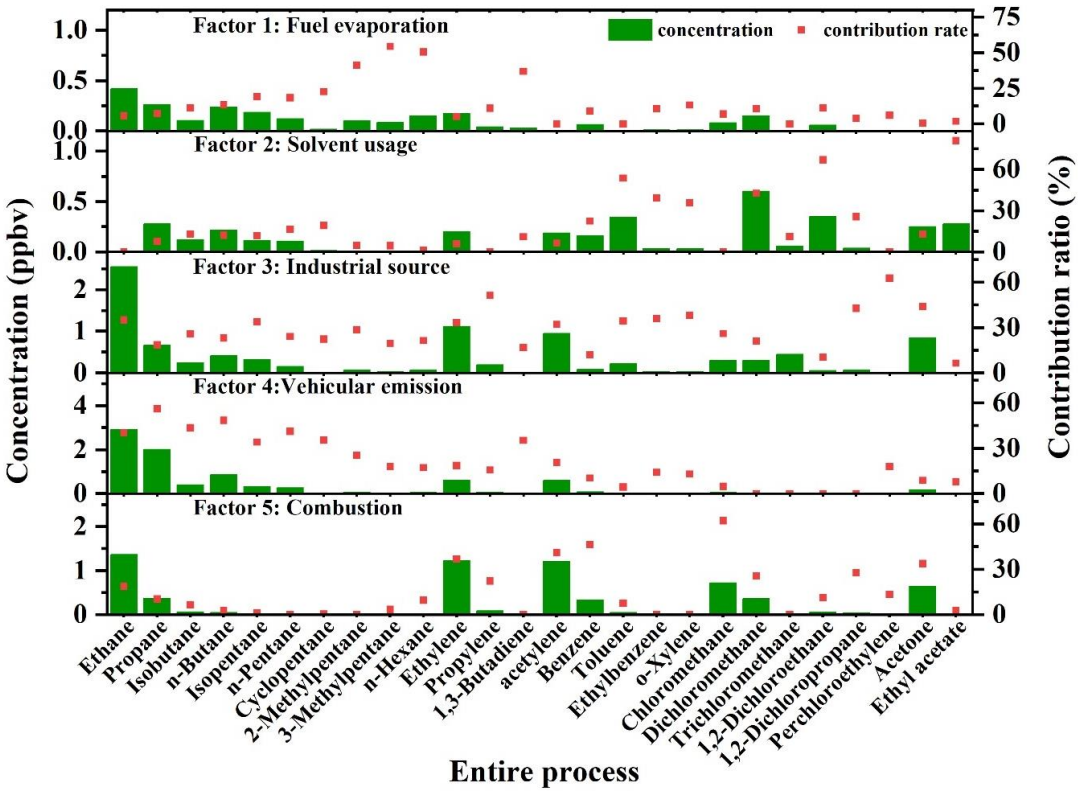

392

393 Fig. 4. Concentration of VOC species in each factor and contribution to each source.

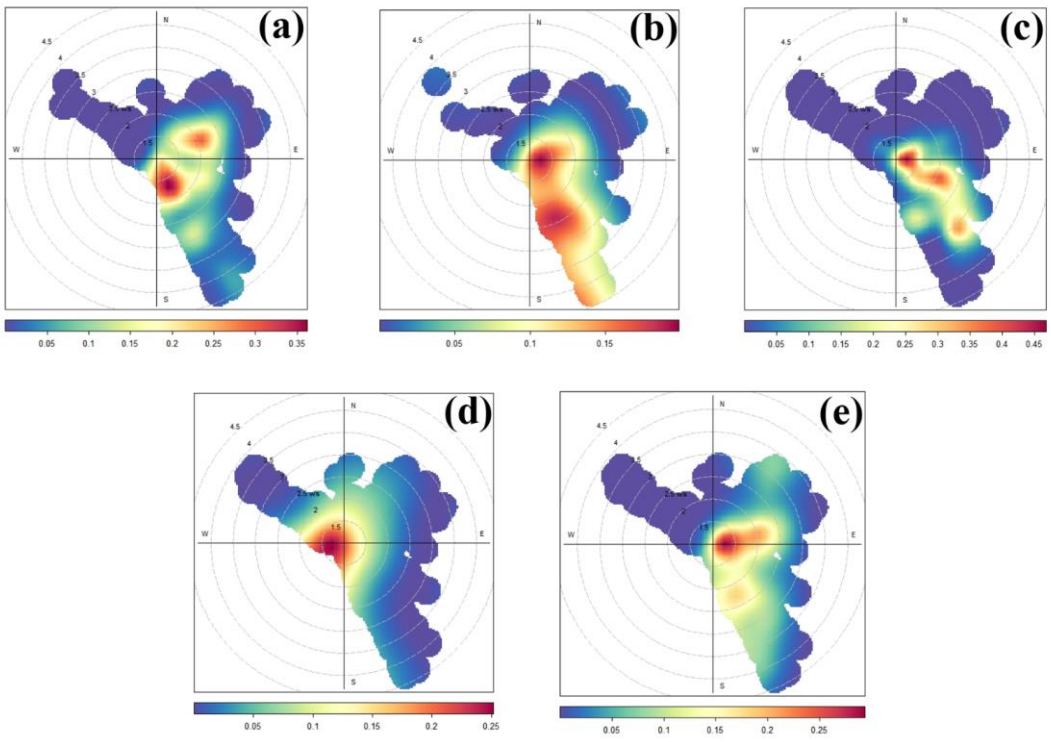

394

395 Fig. 5. CPF plots of five VOCs sources obtained using the PMF model.

Note: a: Fuel evaporation; b: Solvent usage; c: Industrial source; d: Vehicular emission; e: Combustion.

Fig. S6 compares the differences in PMF source profiles between the Omicron infection period and the recovery period, as well as between the pollution day and the clean day. We present the concentrations of the five main VOCs in all five factors in Table S2. Ethane (vehicular emission), 2-methylpentane (fuel evaporation), benzene (industry source), chloromethane (combustion), and ethyl acetate (solvent usage) were selected as tracers for five sources. Ethane concentration in Case 2 (5.9 ppbv) is much higher than in other processes, and ethane concentration during the recovery period (3.4 ppbv) is also higher than during the infection period (2.4 ppbv), which may to some extent reflect increased vehicular emissions during the recovery period.

Concentrations of most species were significantly higher during the recovery period than during the infection period. The representative pollution processes in both periods showed the same results as well, with a 79% higher concentration of TVOCs in Case 2 (65.1 ppbv) compared to Case 1 (36.3 ppbv) (Fig. 6). While in Case 1 industry was the dominant source of VOCs, by Case 2 motorized sources reached a concentration value of 21.2 ppbv, accounting for 33% of the observed VOCs, and became the dominant source of emissions. This is consistent with the fact that people's mobility activities have increased after the epidemic has entered the recovery period. As a group of VOCs species with the highest concentration share, ethane and propane contributed more to the clean days motor vehicle source than other processes, which also resulted in a 34% clean days motor vehicle source share.

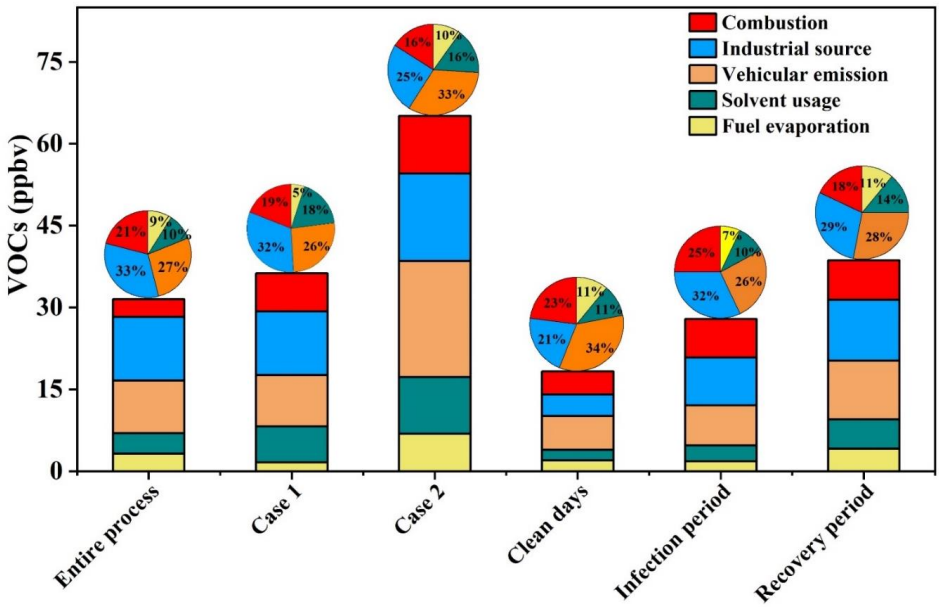

Fig. 6. Contribution of each to VOCs for different processes.

3.3 SOAP

VOCs are estimated to contribute about 16−30% or more of $PM_{2.5}$ by mass through SOA production (Huang et al., 2014). Therefore, by calculating the SOAP value, the influence of different sources on $PM_{2.5}$ production can be reflected to a certain extent.

We have included quantitative analysis for SOAP as well. Fig. 7 shows the SOAP concentrations and contribution rates of the top ten species throughout the entire process, during two pollution processes, and clean days. The top ten species all reached close to 100% of the total SOAP contribution, with Case 1 reaching 98%. In each process, the composition of the top ten substances is essentially the same. Aromatic hydrocarbons contributed the most, with BTEX always occupying the top five positions and toluene the most. The SOAP values of the top ten contributing species for the two polluting processes are shown in Tables S3 and S4. Toluene, the highest contributing species, reached a SOAP value of 49.4 μg/m^3 in the most polluted Case 2, which was 3.2 times higher than the SOAP sum of all species on the clean day (15.5 μg/m^3). The SOAP value for Case 1, which is also a contaminated process, was 67 μg/m^3, and the main species (m/xylene: 9.8 μg/m^3, benzene: 8.5 μg/m^3) including toluene (34.6 μg/m^3) were lower than those for Case 2 (m/xylene: 19.4 μg/m^3, benzene: 13.4 μg/m^3).

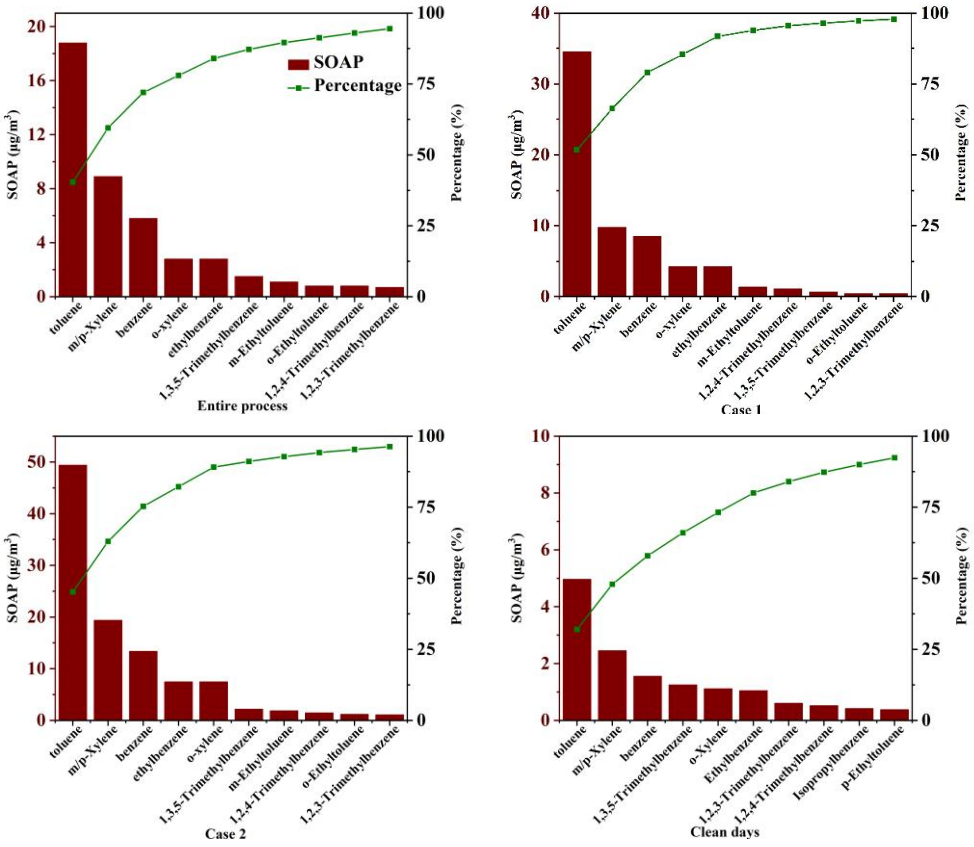

Fig. 7. SOAP dominant species in different processes

Figure 8 shows the SOAP calculated after source resolution of the two pollution processes by PMF for clean days, respectively. In Case 1, industrial source is the dominant source with a contribution ratio of 63%. In Case 2, the pollution sources exhibit a more evenly distributed contribution, where the solvent usage and fuel evaporation sources emerge as the primary contributors to SOAP, with their respective contribution levels rising to 32% and 26%. Case 1 was during the infection period, when social activities had not yet returned to normal. In Case 2, when society had basically returned to normal, the increase in emissions from various sources resulted in a more balanced distribution of SOAP contributions and caused more severe $PM_{2.5}$ pollution. In addition, a few days before Case 2, the Zhengzhou Municipal People's Government initiated the Heavy Pollution Weather Level II response (https://sthjj.zhengzhou.gov.cn/tzgg/7037130.jhtml) and introduced control measures for emissions from industrial and mobile sources, which resulted in a significant reduction of SOAP levels from industrial and motorized sources in Case 2. The clean day result with a SOAP of 8.8 $\mu g/m^3$ also indicates that industrial and solvent usage sources are the most dominant SOAP sources. The primary sources of aromatic compounds, which are the most significant contributors to SOAP, are solvent usage and industrial process emissions. This finding aligns with the results of other studies (Wu et al., 2017). Consequently, it is imperative to implement measures to reduce $PM_{2.5}$ pollution by regulating emissions from industrial and solvent usage sources.

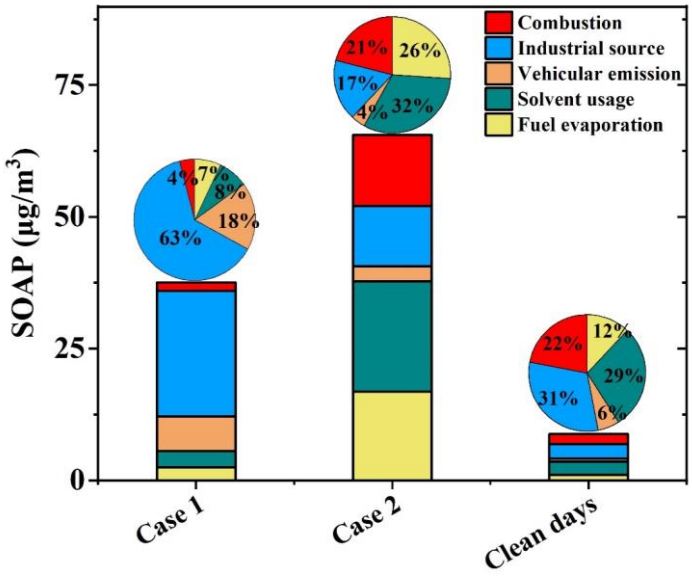

Fig. 8. SOAP value and contribution ratio of each process

4. Conclusions

Continuous observation of VOCs during the infection of the Omicron epidemic was carried out at an urban site in polluted Zhengzhou from December 1, 2022, to January 31, 2023. The daily average concentration of $PM_{2.5}$ ranged from 53.5 to 239.4 μg/m^3 with an average value of 111.5 ± 45.1 μg/m^3 during the whole period. The concentration of TVOCs ranged from 15.6 to 57.1 ppbv with an average of 36.1 ± 21.0 ppbv, higher than the same period in last year (27.9 ± 12.7 ppbv, Lai et al., 2024). Two representative contamination processes were identified (Case 1 during the infection period and Case 2 during the recovery period). The concentration of TVOCs in Case 1 and Case 2 were 48.4 ± 20.4 and 67.6 ± 19.6 ppbv, respectively, increased by 63% and 188% compared with values during clean days. The average concentrations of $PM_{2.5}$ and TVOCs during Case 2 were 1.3 and 1.8 times of the values in Case 1. This is consistent with the observed increase in pollutant emissions following the return to normal social life from the period of Omicron infection. The highest volume contributions of alkanes were found both in Case 1 (48%) and Case 2 (44%). Though the volume contribution of aromatics were the lowest (6% in Case 1 and 7% in Case 2), the highest increase ratio was found from clean days to polluted episodes. Low wind speed and high humidity were the main meteorological reasons for the occurrence of pollution. Analyzing the sources of VOCs revealed that VOCs were found to be affected by a combination of local emissions and regional transport. The primary sources of atmospheric VOCs in Zhengzhou were identified as industrial emissions (32%), vehicle emissions (27%), and combustion (21%). Significant discrepancies were observed in the sources of VOCs between the two pollution processes. In Case 1, industrial emissions constituted the primary source of VOCs, accounting for 32% of the total VOC concentration. In contrast, in Case 2, the proportion of vehicle emissions increased to 33%, representing the primary source of VOCs.

A further analysis of the effect of VOCs on SOA generation reveals that aromatic compounds are the primary contributors to SOAP, with BTEX being the predominant contributor throughout the period. The SOAP values reached 37.6 and 65.6 μg/m³ in Case 1 and Case 2, respectively. In Case 1, the greatest contribution to SOAP was made by industrial sources (63%, 23.8 μg/m³), while vehicular sources, which constituted the second most important source, accounted for only 18%. In Case 2, the contribution of each VOC source was more evenly distributed, with solvent use sources and fuel

evaporation sources representing the primary contributors to SOAP, accounting for 32% (20.9 μg/m³) and 26% (16.8 μg/m³), respectively. The SOAP result for the clean day was 8.8 μg/m³, with industrial sources and solvent use still being the primary contributors. Therefore, the industrial and solvent use sectors are the predominant sources of pollutants during this observation. The aforementioned results substantiate the considerable impact of elevated emissions from all sources on the exacerbation of pollution following the conclusion of the Omicron infection.

Author contribution:

Bowen Zhang: Data curation, Methodology, Formal analysis, Writing Original Draft.
Dong Zhang: Data curation, Formal analysis, Review & Editing.
Zhe Dong: Data curation, Formal analysis, Review & Editing.
Xinshuai Song: Data curation, Formal analysis.
Ruiqin Zhang: Supervision, Writing-Review & Editing, Funding acquisition.
Xiao Li: Formal analysis, Investigation, Supervision, Writing-Review & Editing.

Competing interests:

The contact author has declared that none of the authors has any competing interests.

Acknowledgments:

This research was supported by the Natural Science Foundation of Henan Province (232300421395) and the National Key Research and Development Program of China (2017YFC0212400).

References

An, J., Zhu, B., Wang, H., Li, Y., Lin, X., and Yang, H.: Characteristics and source apportionment of VOCs measured in an industrial area of Nanjing, Yangtze River Delta, China, Atmospheric Environment, 97, 206-214, https://doi.org/10.1016/j.atmosenv.2014.08.021, 2014.

Bai, L., Lu, X., Yin, S., Zhang, H., Ma, S., Wang, C., Li, Y., and Zhang, R.: A recent emission inventory of multiple air pollutant, $PM_{2.5}$ chemical species and its spatial-temporal characteristics in central China, Journal of Cleaner Production, 269, 122114, https://doi.org/10.1016/j.jclepro.2020.122114, 2020.

Buzcu, B. and Fraser, M. P.: Source identification and apportionment of volatile

525 organic compounds in Houston, TX, Atmospheric Environment, 40, 2385-2400,
526 https://doi.org/10.1016/j.atmosenv.2005.12.020, 2006.
527 Conner, T. L., Lonneman, W. A., Seila, R.L.: Transportation-related volatile
528 hydrocarbon source profiles measured in atlanta, Journal of the Air & Waste
529 Management Association, 45 (5), 383-394,
530 https://doi.org/10.1080/10473289.1995.10467370, 1995.
531 Cui, L., Wu, D., Wang, S., Xu, Q., Hu, R., and Hao, J.: Measurement report:
532 Ambient volatile organic compound (VOC) pollution in urban Beijing: characteristics,
533 sources, and implications for pollution control, Atmospheric Chemistry and Physics,
534 22, 11931-11944, https://doi.org/10.5194/acp-22-11931-2022, 2022.
535 Derwent, R. G., Jenkin, M. E., Utembe, S. R., Shallcross, D. E., Murrells, T. P.,
536 and Passant, N. R.: Secondary organic aerosol formation from a large number of
537 reactive man-made organic compounds, Science of the Total Environment, 408, 3374-
538 3381, https://doi.org/10.1016/j.scitotenv.2010.04.013, 2010.
539 Duan, S., Jiang, N., Yang, L., Zhang, R.: Transport Pathways and Potential Sources
540 of $PM_{2.5}$ During the Winter in Zhengzhou, Environmental Science, Jan 8;40(1):86-93,
541 https://doi.org/10.13227/j.hjkx.201805187, 2019.
542 Gao, J., Zhang, J., Li, H., Li, L., Xu, L., Zhang, Y., Wang, Z., Wang, X., Zhang,
543 W., Chen, Y., Cheng, X., Zhang, H., Peng, L., Chai, F., and Wei, Y.: Comparative study
544 of volatile organic compounds in ambient air using observed mixing ratios and initial
545 mixing ratios taking chemical loss into account – A case study in a typical urban area
546 in Beijing, Science of the Total Environment, 628-629, 791-804,
547 https://doi.org/10.1016/j.scitotenv.2018.01.175, 2018.
548 Guan, Y., Liu, X., Zheng, Z., Dai, Y., Du, G., Han, J., Hou, L. a., and Duan, E.:
549 Summer O_3 pollution cycle characteristics and VOCs sources in a central city of
550 Beijing-Tianjin-Hebei area, China, Environmental Pollution, 323, 121293,
551 https://doi.org/10.1016/j.envpol.2023.121293, 2023.
552 Huang, R., Zhang, Y., Bozzetti, C. et al.: High secondary aerosol contribution to p
553 articulate pollution during haze events in China, Nature, 514 (7521), 218−22, https://d
554 oi.org/10.1038/nature13774, 2014.
555 Hui, L., Liu, X., Tan, Q., Feng, M., An, J., Qu, Y., Zhang, Y., Deng, Y., Zhai, R., a
556 nd Wang, Z.: VOC characteristics, chemical reactivity and sources in urban Wuhan, ce
557 ntral China, Atmospheric Environment, 224, 117340, https://doi.org/10.1016/j.atmose
558 nv.2020.117340, 2020.

559 Jensen, A., Liu, Z., Tan, W., Dix, B., Chen, T., Koss, A., Zhu, L., Li, L., de Gouw,
560 J.: Measurements of volatile organic compounds during the COVID-19 lockdown in
561 Changzhou, China, Geophysical research letters, 48(20), https://doi.org/10.1029/2021
562 GL095560, 2021.
563 Jiang, N., Hao, X., Hao, Q., Wei, Y., Zhang, Y., Lyu, Z., Zhang, R.: Changes in se
564 condary inorganic ions in $PM_{2.5}$ at different pollution stages before and after COVID-1
565 9 control, Environmental Science, 44(5), 2430-2440, https://doi.org/10.13227/j.hjkx.2
566 02206170, 2023.
567 Kumar, A., Singh, D., Kumar, K., Singh, B. B., and Jain, V. K.: Distribution of
568 VOCs in urban and rural atmospheres of subtropical India: Temporal variation, source
569 attribution, ratios, OFP and risk assessment, Science of the Total Environment, 613-614,
570 492-501, https://doi.org/10.1016/j.scitotenv.2017.09.096, 2018.
571 Lai, M., Zhang, D., Yin, S., Song, X., and Zhang, R.: Pollution characteristics,
572 source apportionment and activity analysis of atmospheric VOCs during winter and
573 summer pollution in Zhengzhou City, Environmental Science, 4108, 3500-3510,
574 https://doi.org/10.13227/j.hjkx.202001133, 2024.
575 Li, B., Ho, S. S. H., Gong, S., Ni, J., Li, H., Han, L., Yang, Y., Qi, Y., and Zhao,
576 D.: Characterization of VOCs and their related atmospheric processes in a central
577 Chinese city during severe ozone pollution periods, Atmospheric Chemistry and
578 Physics, 19, 617-638, https://doi.org/10.5194/acp-19-617-2019, 2019.
579 Li, J., Deng, S., Tohti, A., Li, G., Yi, X., Lu, Z., Liu, J., and Zhang, S.: Spatial
580 characteristics of VOCs and their ozone and secondary organic aerosol formation
581 potentials in autumn and winter in the Guanzhong Plain, China, Environmental
582 Research, 211, 113036, https://doi.org/10.1016/j.envres.2022.113036, 2022.
583 Li, J., Xie, S. D., Zeng, L. M., Li, L. Y., Li, Y. Q., and Wu, R. R.: Characterization
584 of ambient volatile organic compounds and their sources in Beijing, before, during, and
585 after Asia-Pacific Economic Cooperation China 2014, Atmospheric Chemistry and
586 Physics, 15, 7945-7959, https://doi.org/10.5194/acp-15-7945-2015, 2015.
587 Li, J., Lu, K., Lv, W., Li, J., Zhong, L., Ou, Y., Chen, D., Huang, X., and Zhang,
588 Y.: Fast increasing of surface ozone concentrations in Pearl River Delta characterized
589 by a regional air quality monitoring network during 2006–2011, Journal of
590 Environmental Sciences, 26, 23-36, https://doi.org/10.1016/S1001-0742(13)60377-0,
591 2014.
592 Liu, Y., Li, X., Tang, G., Wang, L., Lv, B., Guo, X., and Wang, Y.: Secondary

593 organic aerosols in Jinan, an urban site in North China: Significant anthropogenic
594 contributions to heavy pollution, Journal of Environmental Sciences, 80, 107-115,
595 https://doi.org/10.1016/j.jes.2018.11.009, 2019.
596 Liu, Y., Shao, M., Fu, L., Lu, S., Zeng, L., and Tang, D.: Source profiles of volatile
597 organic compounds (VOCs) measured in China: Part I, Atmospheric Environment, 42,
598 6247-6260, https://doi.org/10.1016/j.atmosenv.2008.01.070, 2008.
599 Liu, Y., Song, M., Liu, X., Zhang, Y., Hui, L., Kong, L., Zhang, Y., Zhang, C., Qu,
600 Y., An, J., Ma, D., Tan, Q., and Feng, M.: Characterization and sources of volatile
601 organic compounds (VOCs) and their related changes during ozone pollution days in
602 2016 in Beijing, China, Environmental Pollution, 257, 113599,
603 https://doi.org/10.1016/j.envpol.2019.113599, 2020.
604 Liu, Z., Hu, K., Zhang, K., Zhu, S., Wang, M., and Li, L.: VOCs sources and roles
605 in O_3 formation in the central Yangtze River Delta region of China, Atmospheric
606 Environment, 302, https://doi.org/10.1016/j.atmosenv.2023.119755, 2023.
607 Li, X., Wang, S., Hao, J.: Characteristics of volatile organic compounds (VOCs)
608 emitted from biofuel combustion in China, Environmental Science, 32, 3515-3521,
609 2011.
610 Li, Y., Yin, S., Zhang R., Yu, S., Yang, J., and Zhang, D.: Characteristics and source
611 apportionment of atmospheric VOCs at different pollution levels in winter in an urban
612 area in Zhengzhou, Environmental Science, 4108, 3500-3510,
613 https://doi.org/10.13227/j.hjkx.202001133, 2020.
614 Ma, Q., Wang, W., Wu, Y., Wang, F., Jin, L., Song, Y., Han, Y., Zhang, R., Zhang,
615 D.: Haze caused by NO_x oxidation under restricted residential and industrial activities
616 in a mega city in the south of North China Plain, Chemosphere, Volume 305, 135489,
617 https://doi.org/10.1016/j.chemosphere.2022.135489, 2022.
618 Merino, M., Marinescu, M., Cascajo, A., Carretero, J., Singh, D.: Evaluating the
619 spread of Omicron COVID-19 variant in Spain, Future Generation Computer Systems,
620 149, 547-561, https://doi.org/10.1016/j.future.2023.07.025, 2023.
621 Monod, A., Sive, B. C., Avino, P., Chen, T., Blake, D. R., and Sherwood Rowland,
622 F.: Monoaromatic compounds in ambient air of various cities: a focus on correlations
623 between the xylenes and ethylbenzene, Atmospheric Environment, 35, 135-149,
624 https://doi.org/10.1016/S1352-2310(00)00274-0, 2001.
625 Mozaffar, A., Zhang, Y.-L., Fan, M., Cao, F., and Lin, Y.-C.: Characteristics of
626 summertime ambient VOCs and their contributions to O_3 and SOA formation in a

627 suburban area of Nanjing, China, Atmospheric Research, 240, 104923,
628 https://doi.org/10.1016/j.atmosres.2020.104923, 2020.
629 Mu, L., Feng, C., Li, Y., Li, X., Liu, T., Jiang, X., Liu, Z., Bai, H., and Liu, X.:
630 Emission factors and source profiles of VOCs emitted from coke production in Shanxi,
631 China, Environmental Pollution, 335, 122373,
632 https://doi.org/10.1016/j.envpol.2023.122373, 2023.
633 Niu, Y., Yan, Y., Chai, J., Zhang, X., Xu, Y., Duan, X., Wu, J., and Peng, L.: Effects
634 of regional transport from different potential pollution areas on volatile organic
635 compounds (VOCs) in Northern Beijing during non-heating and heating periods,
636 Science of the Total Environment, 836, 155465,
637 https://doi.org/10.1016/j.scitotenv.2022.155465, 2022.
638 Norris, G., Duvall, R., Brown, S., Bai. S. EPA Positive Matrix Factorization (PMF)
639 5.0 Fundamentals and User Guide. U.S. Environmental Protection Agency, Washington,
640 DC, EPA/600/R-14/108 (NTIS PB2015-105147), 2014.
641 Paatero, P., Eberly, S., Brown, S. G., Norris, G. A.: Methods for estimating
642 uncertainty in factor analytic solutions, Atmospheric Measurement Techniques, Volume
643 7, 781-797, https://doi.org/10.5194/amt-7-781-2014, 2014.
644 Pei, C., Yang, W., Zhang, Y., Song, W., Xiao, S., Wang, J., Zhang, J., Zhang, T.,
645 Chen, D., Wang, Y., Chen, Y., Wang, X.: Decrease in ambient volatile organic
646 compounds during the COVID-19 lockdown period in the Pearl River Delta region,
647 south China, Science of The Total Environment, 823, 153720,
648 https://doi.org/10.1016/j.scitotenv.2022.153720, 2022.
649 Petersen, M. S., Í Kongsstovu, S., Eliasen, E. H., Larsen, S., Hansen, J. L., Vest,
650 N., Dahl, M. M., Christiansen, D. H., Møller, L. F., & Kristiansen, M. F.: Clinical
651 characteristics of the Omicron variant - results from a Nationwide Symptoms Survey
652 in the Faroe Islands, International Journal of Infectious Diseases, 122, 636–643,
653 https://doi.org/10.1016/j.ijid.2022.07.005, 2022.
654 Qi, J., Mo, Z., Yuan, B., Huang, S., Huangfu, Y., Wang, Z., Li, X., Yang, S., Wang,
655 W., Zhao, Y., Wang, X., Wang, W., Liu, K., and Shao, M.: An observation approach in
656 evaluation of ozone production to precursor changes during the COVID-19 lockdown,
657 Atmospheric Environment, 262, 118618,
658 https://doi.org/10.1016/j.atmosenv.2021.118618, 2021.
659 Russo, R. S., Zhou, Y., White, M. L., Mao, H., Talbot, R., and Sive, B. C.: Multi-
660 year (2004–2008) record of nonmethane hydrocarbons and halocarbons in New

England: seasonal variations and regional sources, Atmospheric Chemistry and Physics, 10, 4909-4929, https://doi.org/10.5194/acp-10-4909-2010, 2010.

Sahu, L. K., Tripathi, N., Gupta, M., Singh, V., Yadav, R., Patel, K.: Impact of COVID-19 Pandemic lockdown in ambient concentrations of aromatic volatile organic compounds in a metropolitan city of western India, Journal of geophysical research, Atmospheres : JGR, 127(6), https://doi.org/10.1029/2022JD036628, 2022.

Schauer, J., Kleeman, M., Cass, G., Simoneit, B.: Measurement of emissions from air pollution sources.5. C_1-C_{32} organic compounds from gasoline-powered motor vehicles, Environmental Science & Technology, 36, 1169-1180, https://doi.org/10.1021/es0108077, 2002.

Shao, P., An, J., Xin, J., Wu, F., Wang, J., Ji, D., and Wang, Y.: Source apportionment of VOCs and the contribution to photochemical ozone formation during summer in the typical industrial area in the Yangtze River Delta, China, Atmospheric Research, 176-177, 64-74, https://doi.org/10.1016/j.atmosres.2016.02.015, 2016.

Shi, Y., Liu, C., Zhang, B., Simayi, M., Xi, Z., Ren, J., and Xie, S.: Accurate identification of key VOCs sources contributing to O_3 formation along the Liaodong Bay based on emission inventories and ambient observations, Science of the Total Environment, 844, 156998, 10.1016/j.scitotenv.2022.156998, 2022.

Singh, B., Sohrab, S., Athar, M., Alandijany, T., Kumari, S., Nair, A., Kumari, S., Mehra, K., Chowdhary, K., Rahman, S., Azhar, E.: Substantial changes in selected volatile organic compounds (VOCs) and associations with health risk assessments in industrial areas during the COVID-19 Pandemic, Toxics, 11, 165, https://doi.org/10.3390/toxics11020165, 2023a.

Singh, B., Singh, M., Ulman, Y., Sharma, U., Pradhan, R., Sahoo, J., Padhi, S., Chandra, P., Koul, M., Tripathi, P., Kumar, D., Masih, J.: Distribution and temporal variation of total volatile organic compounds concentrations associated with health risk in Punjab, India, Case Studies in Chemical and Environmental Engineering, 8, 100417, https://doi.org/10.1016/j.cscee.2023.100417, 2023b.

Song, M., Li, X., Yang, S., Yu, X., Zhou, S., Yang, Y., Chen, S., Dong, H., Liao, K., Chen, Q., Lu, K., Zhang, N., Cao, J., Zeng, L., and Zhang, Y.: Spatiotemporal variation, sources, and secondary transformation potential of volatile organic compounds in Xi'an, China, Atmospheric Chemistry and Physics, 21, 4939-4958, https://doi.org/10.5194/acp-21-4939-2021, 2021.

Song, X., Zhang, D., Li, X., Lu, X., Wang, M., Zhang, B., Zhang, R.: Simultaneous

observations of peroxyacetyl nitrate and ozone in Central China during static management of COVID-19: Regional transport and thermal decomposition, Atmospheric Research, Volume 294, 106958, https://doi.org/10.1016/j.atmosres.2023.106958, 2023.

Song, Y., Shao, M., Liu, Y., Lu, S., Kuster, W., Goldan, P., and Xie, S.: Source apportionment of ambient volatile organic compounds in Beijing, Environmental Science & Technology, 41, 4348-4353, https://doi.org/10.1021/es0625982, 2007.

Wang, H., Li, J., Peng, Y., Zhang, M., Che, H., Zhang, X.: The impacts of the meteorology features on $PM_{2.5}$ levels during a severe haze episode in central-east China, Atmospheric Environment, Volume 197, Pages 177-189, ISSN 1352-2310, https://doi.org/10.1016/j.atmosenv.2018.10.001, 2019.

Wang, H., Wang, Q., Chen, J. Chen, C., Huang, C., Qiao, L. Lou, S., Lu, J.: Do vehicular emissions dominate the source of C6–C8 aromatics in the megacity Shanghai of eastern China?, Environmental Science, 27, 290-297, https://doi.org/10. 1016/j.jes.2014.05.033, 2015.

Wang, M., Lu, S., Shao, M., Zeng, L., Zheng, J., Xie, F., Lin, H., Hu, K., and Lu, X.: Impact of COVID-19 lockdown on ambient levels and sources of volatile organic compounds (VOCs) in Nanjing, China, Science of the Total Environment, 757, 143823, https://doi.org/10.1016/j.scitotenv.2020.143823, 2021.

Wang, M., Zeng, L., Lu, S., Shao, M., Liu, X., Yu, X., Chen, W., Yuan, B., Zhang, Q., Hu, M., & Zhang, Z.: Development and validation of a cryogen-free automatic gas chromatograph system (GC-MS/FID) for online measurements of volatile organic compounds, Analytical Methods, 6, 9424, https://doi.org/10.1039/C4AY01855A, 2014.

Wang, T., Xue, L., Brimblecombe, P., Lam, Y. F., Li, L., and Zhang, L.: Ozone pollution in China: A review of concentrations, meteorological influences, chemical precursors, and effects, Science of the Total Environment, 575, 1582-1596, https://doi.org/10.1016/j.scitotenv.2016.10.081, 2017.

Wu, R., Li, J., Hao, Y., Li, Y., Zeng, L., and Xie, S.: Evolution process and sources of ambient volatile organic compounds during a severe haze event in Beijing, China, Science of the Total Environment, 560-561, 62-72, https://doi.org/10.1016/j.scitotenv.2016.04.030, 2016.

Wu, W., Zhao, B., Wang, S., and Hao, J.: Ozone and secondary organic aerosol formation potential from anthropogenic volatile organic compounds emissions in China, Journal of Environmental Sciences, 53, 224-237,

https://doi.org/10.1016/j.jes.2016.03.025, 2017.

Xiong, Y., Zhou, J., Xing, Z., and Du, K.: Optimization of a volatile organic compound control strategy in an oil industry center in Canada by evaluating ozone and secondary organic aerosol formation potential, Environmental Research, 191, 110217, https://doi.org/10.1016/j.envres.2020.110217, 2020.

Yu, F., Wang, Q., Yan, Q., Jiang, N., Wei, J., Wei, Z., Yin, S.: Particle size distribution, chemical composition and meteorological factor analysis: A case study during wintertime snow cover in Zhengzhou, China, Atmospheric Research, 202, 140-147, 0169-8095, https://doi.org/10.1016/j.atmosres.2017.11.016, 2018.

Yun, L., Li, C., Zhang, M., He, L. and Guo, J.: Pollution characteristics and sources of atmospheric VOCs in the coastal background area of the Pearl River Delta, Environmental Science, 4191-4201, https://doi.org/10.13227/j.hjkx.202101155, 2021.

Zeng, X., Han, M., Ren, G., Liu, G., Wang, X., Du, K., Zhang, X., and Lin, H.: A comprehensive investigation on source apportionment and multi-directional regional transport of volatile organic compounds and ozone in urban Zhengzhou, Chemosphere, 334, 139001, https://doi.org/10.1016/j.chemosphere.2023.139001, 2023.

Zhang, C., Liu, X., Zhang, Y., Tan, Q., Feng, M., Qu, Y., An, J., Deng, Y., Zhai, R., Wang, Z., Cheng, N., and Zha, S.: Characteristics, source apportionment and chemical conversions of VOCs based on a comprehensive summer observation experiment in Beijing, Atmospheric Pollution Research, 12, 230-241, https://doi.org/10.1016/j.apr.2020.12.010, 2021a.

Zhang, D., He, B., Yuan, M., Yu, S., Yin, S., and Zhang, R.: Characteristics, sources and health risks assessment of VOCs in Zhengzhou, China during haze pollution season, Journal of Environmental Sciences, 108, 44-57, https://doi.org/10.1016/j.jes.2021.01.035, 2021b.

Zhang, D., Li, X., Yuan, M., Xu, Y., Xu, Q., Su, F., Wang, S., Zhang, R.: Characteristics and sources of nonmethane volatile organic compounds (NMVOCs) and O_3–NO_x–NMVOC relationships in Zhengzhou, China, Atmosphere Chemistry and Physics, 24, 8549-8567, https://doi.org/10.5194/acp-24-8549-2024, 2024.

Zhang, F., Shang, X., Chen, H., Xie, G., Fu, Y., Wu, D., Sun, W., Liu, P., Zhang, C., Mu, Y., Zeng, L., Wan, M., Wang, Y., Xiao, H., Wang, G., and Chen, J.: Significant impact of coal combustion on VOCs emissions in winter in a North China rural site, Science of the Total Environment, 720, 137617, https://doi.org/10.1016/j.scitotenv.2020.137617, 2020.

763 Zhang, J., Sun, Y., Wu, F., Sun, J., and Wang, Y.: The characteristics, seasonal
764 variation and source apportionment of VOCs at Gongga Mountain, China, Atmospheric
765 Environment, 88, 297-305, https://doi.org/10.1016/j.atmosenv.2013.03.036, 2014.
766 Zhang, Z., Yan, X., Gao, F., Thai, P., Wang, H., Chen, D., Zhou, L., Gong, D., Li,
767 Q., Morawska, L., and Wang, B.: Emission and health risk assessment of volatile
768 organic compounds in various processes of a petroleum refinery in the Pearl River Delta,
769 China, Environmental Pollution, 238, 452-461,
770 https://doi.org/10.1016/j.envpol.2018.03.054, 2018.
771 Zheng, H., Kong, S., Xing, X., Mao, Y., Hu, T., Ding, Y., Li, G., Liu, D., Li, S.,
772 and Qi, S.: Monitoring of volatile organic compounds (VOCs) from an oil and gas
773 station in northwest China for 1 year, Atmospheric Chemistry and Physics, 18, 4567-
774 4595, https://doi.org/10.5194/acp-18-4567-2018, 2018.
775 Zheng, J., Zhong, L., Wang, T., Louie, P. K. K., and Li, Z.: Ground-level ozone in
776 the Pearl River Delta region: Analysis of data from a recently established regional air
777 quality monitoring network, Atmospheric Environment, 44, 814-823,
778 https://doi.org/10.1016/j.atmosenv.2009.11.032, 2010.
779 Zhou, Z., Xiao, L., Fei, L., Yu, W., Lin M., Huang, T., Zhang, Z. and Tao J.:
780 Characteristics and sources of VOCs during ozone pollution and non-pollution periods
781 in summer in Dongguan industrial concentration area, Environmental Science, 4497-
782 4505, https://doi.org/10.13227/j.hjkx.202111285, 2022.
783 Zou, Y., Yan, X. L., Flores, R. M., Zhang, L. Y., Yang, S. P., Fan, L. Y., Deng, T.,
784 Deng, X. J., and Ye, D. Q.: Source apportionment and ozone formation mechanism of
785 VOCs considering photochemical loss in Guangzhou, China, Science of the Total
786 Environment, 903, 166191, https://doi.org/10.1016/j.scitotenv.2023.166191, 2023.
787 Zuo, H., Jiang, Y., Yuan, J., Wang, Z., Zhang, P., Guo, C., Wang, Z., Chen, Y., Wen,
788 Q., Wei, Y., Li, X.: Pollution characteristics and source differences of VOCs before and
789 after COVID-19 in Beijing, Science of The Total Environment, 907, 167694,
790 https://doi.org/10.1016/j.scitotenv.2023.167694, 2024.

791